New Approach for Determining the Conformational Features of Pseudorotating Ring Molecules Utilizing Calculated and Measured NMR Spin−Spin Coupling Constants

Anan Wu and Dieter Cremer*

Department of Theoretical Chemistry, Göteborg University, Reutersgatan 2, S-41320 Göteborg, Sweden

Received: October 22, 2002; In Final Form: December 2, 2002

A new method is developed to determine the most stable conformations of puckered rings by a comparison of measured and calculated SSCCs (DORCO: determination of ring conformations). The DORCO method extensively uses the ring puckering coordinates to express the properties of a pseudorotating puckered ring. In the case of NMR spin−spin coupling constants (SSCCs) J, this leads to an extension of the Karplus relationship to puckered rings. For five-membered rings with puckering coordinates q and ϕ, the Karplus relationships adopt the form ${}^nJ(q,\phi)$ or ${}^nJ(\phi)$. It is shown in this paper that functions ${}^3J(\mathrm{HCCH})(\phi)$ calculated with coupled perturbed density functional theory for a parent molecule can also be used for derivatives of the parent molecule and help to determine their conformational probability distribution function $\rho(\phi)$. For this purpose, the DORCO procedure is developed to use functions ${}^nJ(\phi)$ of the parent molecule in connection with measured SSCCs of the substituted compound. DORCO was tested for tetrahydrofuran and two of its derivatives. The most stable conformations were determined by an accuracy of 4% or better.

1. Introduction

Nuclear magnetic resonance spectroscopy (NMR) is a powerful tool for determining the conformation of biochemically interesting molecules as has been documented in many research articles and reviews.[1−4] One important tool in this connection is the well-known dependence of the spin−spin coupling constant (SSCC) on the conformational coordinates of a molecule as was first exploited by Karplus.[5,6] He established trigonometric relationships between vicinal coupling constants of the type HCCH and the dihedral angle of the HCCH unit. These so-called Karplus relationships were later generalized for a multitude of vicinal SSCCs including heteroatoms and various types of substituents.[7]

The generalization of the Karplus relationship to ring molecules bears a number of problems as will be discussed in this work. We will show that these problems can elegantly be circumvented by using a set of conformational parameters for the ring molecule that is uniquely defined. With the help of these coordinates, more general Karplus relationships can be given for all SSCCs of a ring molecule, i.e., not just for vicinal but also one-bond, geminal, and long-range SSCCs. Once the functional form of these Karplus relationships is established, they can be used to determine conformational features of a ring molecule by an approach developed in this paper. This work will describe the theoretical basis of this approach and will demonstrate its usefulness for conformational studies of ring molecules selecting tetrahydrofuran (THF) and its derivatives as suitable examples.

An essential feature of the new approach is the reliable calculation of SSCCs with the help of coupled perturbed density functional theory (CP-DFT) as recently described by Sychrovsky, Gräfenstein, and Cremer.[8] These authors showed that all four contributions to the indirect isotropic SSCCs, namely, the Fermi contact (FC), paramagnetic spin−orbital (PSO), diamagnetic spin−orbit (DSO), and spin-dipole (SP) contribution, are reliably determined at the CP-DFT level of theory using a hybrid functional such as B3LYP[9] (for related work, see also ref 10). Hence, we will use CP-DFT/B3LYP to calculate the SSCCs of various ring molecules. The combination of calculated and measured SSCCs will lead to a *d*etermination *o*f *r*ing *c*onformations (DORCO method) which are most stable and most populated under the conditions of the experimental measurement.

2. Basic Theory

In the following, we shortly summarize the theory of ring puckering coordinates as originally developed by Cremer and Pople[11] and later expanded and applied by Cremer in various articles and reviews.[12−18] The Cremer−Pople theory is based on a definition of a mean plane of the ring, which can be considered as the plane of the planar ring. The out-of-plane displacements of a puckered ring from this reference plane are determined by $N-3$ puckering coordinates $\{q_m,\phi_m\}$, which are related to the unique set of $N-3$ out-of-plane vibrations of the planar N-membered ring. The set $\{q_m,\phi_m\}$ can be partitioned into sets of $(N-3)/2$ (N being odd) pseudorotational coordinates spanning two-dimensional subspaces and (only for N being even) an additional single inversion coordinate $q_{N/2}$. The pseudorotational coordinates are the puckering amplitudes q_m describing the degree of ring puckering in the mth pseudorotational mode and the pseudorotational phase angle ϕ_m describing the mode of ring puckering for pseudorotation m. In the case of a five-membered ring, there exists just one pair q,ϕ of pseudorotational coordinates ($m=2$ can be dropped here), and therefore, the calculation of the out-of-plane coordinates z_j depends only on q and ϕ:

$$z_j=\left(\frac{2}{5}\right)^{1/2} q\cos\left[\frac{4\pi(j-1)}{5}+\phi\right] \text{ for } j=1,\ldots,5 \text{ and } \phi[0;2\pi] \tag{1}$$

where the coordinates z_j are normalized according to

$$\sum_{j=1}^{5} z_j^{\,2}=q^2 \tag{2}$$

* To whom correspondence should be addressed.

10.1021/jp022277m CCC: $25.00
Published on Web 02/25/2003

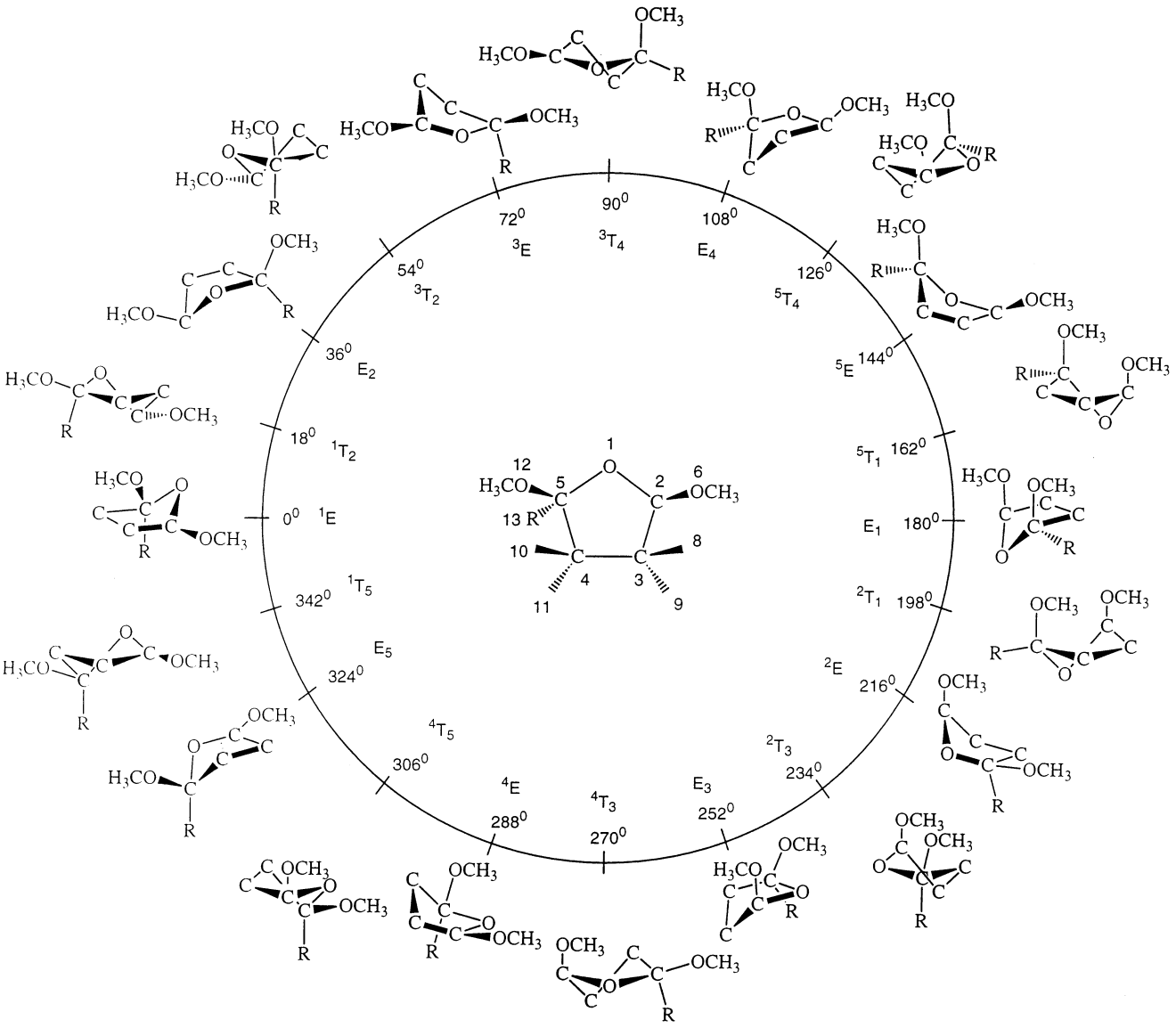

Figure 1. Pseudorotation itinerary ($\phi = 0 \rightarrow 360°$) of *cis*-2,5-dimethoxy-tetrahydrofuran as indicated by the 10 envelope (E) and 10 twist (T) forms at $\phi = (0 + k360)/10$ and $\phi = (18 + k360)/10$ ($k = 0, 1, 2, ..., 9$), respectively. At the center ($q = 0$), the planar ring is located. The position of the methoxy group in the case of *trans*-2,5-dimethoxy-tetrahydrofuran is indicated by the symbol R.

Similar equations were derived by Cremer and Pople for larger puckered rings.[11,12] Once the out-of-plane coordinates for a given five-membered ring conformation are known, coordinates *x,y* can be calculated from *N* ring bond lengths and $N - 3$ internal ring bond angles according to a procedure described elsewhere.[14]

There is an infinite number of puckered ring conformations along the pseudorotation itinerary of a ring molecule such as THF. However, it is useful to select out of these conformations a subset of 20 forms, which correspond to the envelope (E) and twist (T) form of the cyclopentane ring. The E forms are located at $\phi = (0 + k360)/10$ ($k = 0, 1, 2, ..., 9$) and the T forms at $\phi = (18 + k360)/10$ ($k = 0, 1, 2, ..., 9$) as is shown in Figure 1 where methoxy substituents are attached to the THF ring to distinguish between symmetry-equivalent THF forms and show pseudorotation in the case of a substituted ring compound. The exact location of each form is given by the numbering of the ring atoms O1, C2, etc. in a clockwise fashion through the ring. The forms shown in Figure 1 provide a qualitative picture of ring pseudorotation, which causes the maximum out-of-plane coordinate to rotate through the ring without leading to an angular momentum of the molecule. Ring inversion proceeds through the planar THF form located in the center of the diagram at $q = 0$.

The different E and T forms shown in Figure 1 are uniquely defined by the value of the pseudorotational angle ϕ. Experimentalists often use an alternative notation of ring conformations based on suitable reference planes taken from the E (atoms 2−5) and the T form (atoms 1, 2, 5) of cyclopentane. Ring atoms, which lie above the reference plane, are written as superscripts and precede the conformational symbol E or T, whereas ring atoms, which lie below the reference plane, are written as subscripts and follow the symbol E and T. This notation is also given in Figure 1. For any puckered ring form, each external ring bond can be identified as being more axially or more equatorially oriented according to definitions given by Cremer.[13] This helps the identification and description of stereoelectronic effects active in a ring molecule such as THF.

The use of the ring puckering coordinates has a number of advantages of which only two are mentioned here. (a) The geometry of any puckered ring form with a given value of ϕ (or q and ϕ) can be optimized even if this form does not occupy a stationary point of the CES. This would not be possible when

using Cartesian or internal coordinates.[14] (b) Any property P (energy, internal coordinates, dipole moment, charge distribution, frequencies, and magnetic properties) of a puckered ring undergoing pseudorotation can be described in terms of the puckering coordinates. For this purpose, P is expanded in a Fourier series of the pseudorotational phase angle ϕ in the case of a five-membered ring (similar formulas apply to N-membered rings):

$$P(q,\phi) = \sum_{k=0}^{\infty}\{P_k^c(q)\cos(k\phi) + P_k^s(q)\sin(k\phi)\} \quad (3a)$$

where the Fourier coefficients P_k^c and P_k^s are in turn expressed as power series in the puckering amplitude q:

$$P_k(q) = \sum_{l=0}^{\infty} P_{kl}\, q^l \quad (3b)$$

For $q = 0$, all but a constant term P_{00}^c vanish. Depending on the symmetry of the five-membered ring in question, eq 3 can be simplified by using selected trigonometric terms keeping $k \leq 3$ and truncating the power series after the quadratic or quartic term. Often it is useful to investigate the changes in the property P just along the pseudorotational path. In this case, eq 3 simplifies to eq 4

$$P(\phi) = \sum_{k=0}^{\infty}(A_k\cos(k\phi) + B_k\sin(k\phi)) \quad (4a)$$

which according to the symmetry of the ring molecule in question and the required accuracy can be simplified to

$$P(\phi) = A_0 + \sum_{i=1}^{c}(A_i\cos(i\phi) + \sum_{j=1}^{s} B_j\sin(j\phi)) \quad (4b)$$

where s and c are the truncation limits. For a free or slightly hindered pseudorotor molecule, experimentally, only a property value averaged over the pseudorotational mode can be measured. In general, each measured property is an average over all vibrational modes. The latter however are usually small amplitude vibrations; stronger vibrational effects can be expected from the large amplitude vibrations. In the five-membered ring, the q vibration (leading to a change in the z_j coordinates for a fixed value of ϕ) is also a large amplitude vibration in case of a small inversion barrier. In the present case, we neglect this and focus exclusively on the pseudorotational mode of the ring; that is, we consider just eq 4. If the functional form of (4) is known, the value of $\langle P\rangle$ averaged over the pseudorotational motion is given by

$$\langle P\rangle = \int_0^{2\pi} \rho(\phi)\, P(\phi)\, \mathrm{d}\phi \quad (5)$$

where the conformational probability distribution $\rho(\phi)$ is defined as a Boltzmann distribution

$$\rho(\phi) = \frac{\mathrm{e}^{-[V(\phi)-V(0)]/RT}}{\int_0^{2\pi}\mathrm{e}^{-[V(\phi)-V(0)]/RT}\,\mathrm{d}\phi} \quad (6)$$

Alternatively, we can express the conformational probability distribution $\rho(\phi)$ in the same functional form as any other ring property P

$$\rho(\phi) = \sum_{i=0}^{c}(C_i\cos(i\phi) + D_i\sin(i\phi)) \quad (7)$$

which is obtained by expanding the exponential terms in eq 6 in a power series and inserting the function $V(\phi)$ in a form similar to eq 3.

Insertion of eqs 4 and 7 into eq 5 and integration leads to a simple expression for $\langle P\rangle$ that contains products of the Fourier expansion coefficients of $P(\phi)$ and $\rho(\phi)$

$$\langle P\rangle = A_0 + \pi\sum_{i=1}^{c}(A_i{*}C_i + B_i{*}D_i) \quad (8)$$

Provided average values $\langle P_\alpha\rangle$ have been measured for a number of ring properties P_α and the functional form $P_\alpha(\phi)$ (i.e., coefficients A_i and B_i in eq 4) is known for each of these properties, then it is possible to determine the unknown coefficients C_i and D_i and, by this, the conformational probability distribution function $\rho(\phi)$, by which the most stable conformation(s) of a puckered ring can be identified. This procedure however will only be useful if a number of requirements are fulfilled:

(1) It must be possible to measure the properties $\langle P_\alpha\rangle$ easily and accurately. This requirement is normally not fulfilled in the case of geometrical parameters. Better suited are spectroscopic data such as rotational constants, vibrational frequencies, infrared intensities, etc. Even better suited are magnetic properties such as NMR chemical shifts and NMR SSCCs. In this work, we choose the latter because they strongly vary with the pseudorotation of the ring.

(2) It is preferable to determine the functional form of $P_\alpha(\phi)$, eq 4, with the help of quantum chemical calculations because this is normally faster and can be improved (if needed) by enhancing the number of calculated property points along the pseudorotational path and by using more accurate quantum chemical methods. Again, the NMR SSCCs turn out to be suitable properties in this connection because their calculation with the CP-DFT method developed by Cremer and co-workers[8] is both economic and reliable.

(3) If functions $P_\alpha(\phi)$ are known for a parent compound A and a sufficiently large number of $\langle P_\alpha\rangle$ values has been measured for a derivative X of the parent compound A, it will be a priori not clear whether $P_\alpha(\phi)$ of A is also valid for X. Considering the fact that the CES of X may differ from that of A because of significant substituent-ring and substituent−substituent interactions, then a recalculation of $P_\alpha(\phi)$ for X may be desirable. However, this would reduce the usefulness of the method suggested in this work. Again, the choice of SSCCs as conformation determining properties turns out to be useful. We will show in this work that despite of substantial substituent effects, the general form of the Karplus relationship of a given SSCC determined for compound A is largely retained for derivatives X.

In view of conditions 1−3, we will determine

$$\langle {}^nJ\rangle = A_0 + \pi\sum_{i=1}^{c}A_i{*}C_i + \pi\sum_{j=1}^{s}B_j{*}D_j \quad (9)$$

where the Fourier expansion coefficients A_i and B_i are taken from

$${}^nJ(\phi) = A_0 + \sum_{i=1}^{c}(A_i\cos(i\phi) + \sum_{j=1}^{s} B_j\sin(j\phi)) \quad (10)$$

The determination of the probability distribution $\rho(\phi)$ must be done under the constraints (11a) and (11b)

$$\rho(\phi) = \sum_{i=0}^{s}(C_i \cos(i\phi) + D_i \sin(i\phi)) \geq 0 \; \phi[0;2\pi] \qquad (11a)$$

$$\int_0^{2\pi} \rho(\phi)\, d\phi = 1 \qquad (11b)$$

In addition, $\rho(\phi)$ must comply with the symmetry of the CES of the given molecule X. Test calculations show that, in particular, constraint (11a) is paramount to avoid unphysical distribution functions with $\rho(\phi) < 0$. Actually, unconstrained optimizations of $\rho(\phi)$ lead to a seemingly better description of the probability maxima, however, they lead also to false additional probability maxima and/or unwanted oscillations in $\rho(\phi)$.

The DORCO method described above differs significantly from conventional approaches for analyzing the conformation of a ring molecule on the basis of NMR data. The latter use the traditional Karplus equation and nonlinear fitting procedures to determine the puckering parameters by assuming a conformational equilibrium between two discrete states.[19] Such an approach has disadvantages as was pointed out by Džakula and co-workers.[20] It suffers also from the fact that a traditional Karplus equation in terms of ring dihedral angles or approximate pseudorotational coordinates leads to significant inaccuracies.[18] Compared to more advanced methods such as the CUPID method proposed by Džakula and co-workers,[20,21] the present method has several advantages that facilitate its use.

(1) All quantities are expressed as periodic functions of ϕ (or in general of all puckering coordinates), which simplifies the identification of a given conformation with the help of NMR measurements. (2) The probability distribution in a larger region of the conformational space is investigated rather than just two conformational forms with competing stabilities. (3) The method can be applied to any puckered *N*-membered ring contrary to other methods that are constrained to five-membered rings. (4) The linear regression analysis guarantees the best possible fit. The Fourier coefficients of the distribution given in eq 11 are unique and linearly independent. (5) In contrast to other approaches, which are limited to vicinal coupling constants, all SSCCs sensitive to conformational changes can be used in the approach described. This simply results from the fact that each property of the puckered ring molecule (internal coordinates, dipole moment, vibrational frequencies, etc.) is described as a function of the puckering coordinates. By this, the dependence of a given SSCC *J* on any geometrical parameter or electronic factor is automatically covered; that is, *J* is also a function of the puckering coordinates. In previous methods, such a dependence had to be derived in each case newly. (6) The use of the CP-DFT for calculating the SSCCs makes the present method flexible and applicable to any ring compound, for which a sufficiently large number of $\langle {}^nJ \rangle$ values has been measured.

3. Computational Methods

THF and its derivatives *cis*- and *trans*-2,5-dimethoxytetrahydrofuran were investigated using DFT with the hybrid functional B3LYP[9] and Pople's 6-31G(d,p) basis set.[22] For the purpose of testing DFT results, THF was also calculated using second-order many-body perturbation theory [MBPT(2)] with the Møller−Plesset(MP) perturbation operator[23] and Dunning's cc-pVTZ basis set.[24]

Geometries of the ring conformations were calculated with the help of analytical gradients for ring puckering coordinates as developed by Cremer.[14] These were also used to calculate vibrational frequencies and to determine zero-point energies (ZPE), thermochemical corrections, and enthalpies at 298 K, *H*(298). In the case of the B3LYP frequency calculations, an ultrafine pruned (99 590) grid was used. When calculating the vibrational contributions to enthalpies, large amplitude vibrations corresponding to the ring puckering modes were treated separately similar to the way internal rotations are treated.[25]

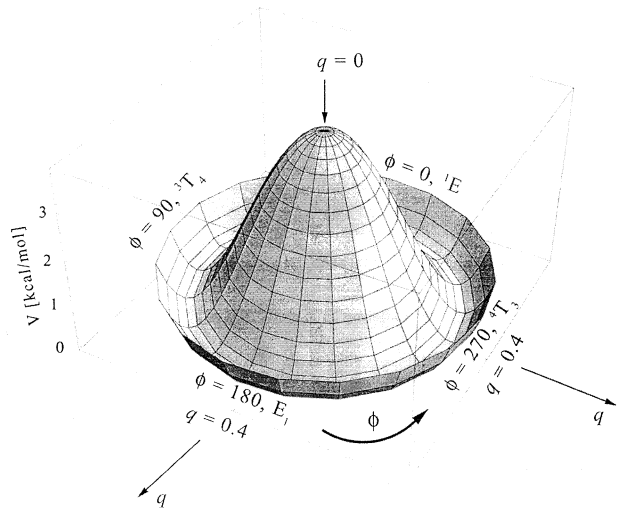

Figure 2. Perspective drawing of the three-dimensional conformational energy surface $V(q,\phi)$ of THF. The planar form with $q = 0$ is located at the maximum. The direction of radial coordinate q and the angular coordinate ϕ is indicated. The minimum energy conformations are found for $q = 0.371$ Å.

CP-DFT was used to calculate the four contributions to the indirect isotropic SSCCs as recently described and implemented by Cremer and co-workers.[8] Previous investigations[8,10,18] revealed that reliable SSCC values are calculated with the B3LYP functional and Kutzelnigg's (9s,5p,1d/5s,1p)[6s,4p,1d/3s,1p] basis.[26] For the calculation of ${}^nJ(q,\phi)$ surfaces according to eq 3 ($P = J$), the following procedure was employed. The CES of THF was scanned by fixing the puckering amplitude q to 0.33, 0.35, 0.39, and 0.41 Å and repeating the geometry optimization of the six unique E and T forms of THF along the pseudorotation itinerary. These calculations were all done at the B3LYP/6-31G(d,p) level of theory. For the optimized THF forms, the calculation of the SSCCs was repeated, and then, all data points of a given SSCC were fitted with the help of eq 3.

In the following, we will simplify the notation of SSCCs by using symbols such as ${}^3J$(HCCH, cis) where C and H denote ^{13}C and ^{1}H, the major coupling path H−C−C−H of the 3-bond SSCC is given, and cis identifies the positions of the H atoms on the same side of the ring.

For the quantum chemical calculations, the program systems COLOGNE2002[27] and Gaussian98[28] were used.

4. Karplus Relationships for the Vicinal Proton−Proton Coupling Constants of Puckered Rings

Both MBPT(2) and B3LYP provide reasonable descriptions of the geometry and the CES of the two ring molecules. Results for cyclopentane were published recently.[18] Those for THF are shortly discussed here in the way they are needed for a better understanding of calculated SSCCs. In Figure 2, the calculated pseudorotational surface of THF is shown, which reveals that THF similar to cyclopentane is essentially a free pseudorotor. The T forms at 90 and 270° represent the most stable conformations of THF, whereas the barrier to pseudorotation

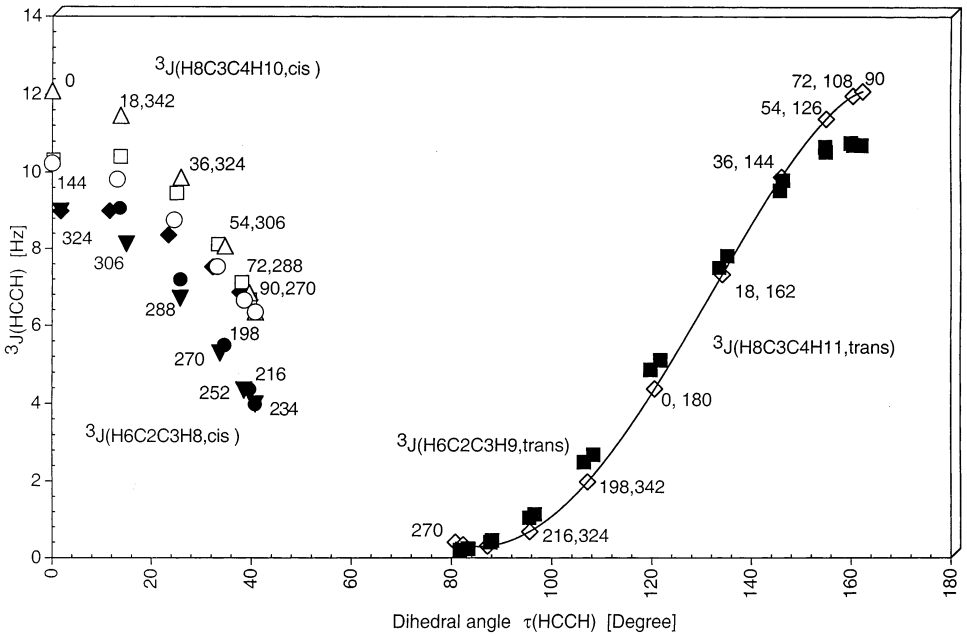

Figure 3. Dependence of the calculated SSCCs ^3J(HCCH) of THF (H6C2C3H8 values are indicated by the following symbols: filled circles, open squares, filled diamonds, filled inverted triangles; H6C2C3H9: filled squares; H8C3C4H10: open triangles, open circles; H8C3C4H11: open diamonds) on the dihedral angle τ(HCCH) according to the traditional Karplus relationship. For each SSCC, the corresponding ϕ value is also given (compare with Figure 1).

TABLE 1: Karplus Relationships $^nJ(\phi)$ Calculated for THF and Average SSCCs $\langle ^nJ\rangle$ of THF and Cyclopentane[a]

parameter	definition	A_0	A_1 cos ϕ	A_2 cos 2ϕ	A_3 cos 3ϕ	A_4 cos 4ϕ	A_5 cos 5ϕ	B_1 sin ϕ	B_2 sin 2ϕ	B_3 sin 3ϕ	STD	$\langle ^nJ\rangle^b$ THF	calc. $\langle ^nJ\rangle$ cyclopentane
^1J(CH)	C2H6	142.57	3.03	−0.38	−0.06	0.04	0.03	1.91	0.77	0.03	0.04	142.60 (144.6)	127.61
^1J(CH)	C3H8	130.89	1.01	0.26	−0.05		0.02	−2.09	−0.01	0.07	0.04	130.88 (132.2)	127.61
^1J(CC)	C3C4	34.35		1.83							0.02	34.23	34.05
^1J(CC)	C2C3	34.06		0.43		−0.01			0.28		0.02	34.04	34.05
^1J(OC)	O1C2	26.41		−0.16		−0.01			0.19		0.04	26.42	
^2J(CC)	C2O1C5	0.87		0.52		0.07					0.00_4	0.84	2.33
^2J(CC)	C2C3C4	0.41		−0.83		0.03			0.50		0.04	0.47	2.33
^2J(OC)	O1C2C3	0.22		−0.69		0.05			0.14		0.02	0.27	
^2J(OH)	O1C2H6	−8.62	−4.96	0.54	0.43	−0.02	−0.02	−1.74	−0.01	0.31	0.02	−8.65	
^2J(CH)	C2C3H8	−1.52	−1.44	−0.22	−0.21	−0.02		−3.00	−0.10	−0.10	0.00_7	−1.50	−2.58
^2J(CH)	C3C2H6	−0.64	−0.64	0.49	0.20	−0.04		0.11	0.23	0.04	0.03	−0.67	−2.58
^2J(CH)	C3C4H10	−2.76	−0.60		−0.06	0.02	0.01	0.39	−0.31	0.16	0.01	−2.76	−2.58
^2J(HH)	H6C2H7	−8.78		−0.45		0.03			−0.07		0.05	−8.75	−12.41
^2J(HH)	H8C3H9	−12.03		−0.03		−0.02			0.26		0.05	−12.03	−12.41
^3J(OH)	O1C2C3H8	−1.20	0.95	0.25	0.06	0.07	0.02	1.80	−0.55	0.25	0.04	−1.21	
^3J(CH)	C2C3C4H10	2.92	−0.31	−1.15	−0.20	−0.08	−0.03	3.85	−0.17	0.39	0.05	2.99	3.92
^3J(CH)	C2O1C5H12	4.12	5.54	1.26	−0.33	0.02		−2.12	−1.14	0.52	0.07	4.04	3.92
^3J(CH)	C4C3C2H6	2.95	2.34	0.30	0.06	0.03	0.01	2.10	1.88	−0.38	0.02	2.93	3.92
^3J(HH)	H6C2C3H8	7.37	0.42	0.54	0.16	−0.12		1.50	−2.09	0.08	0.03	7.33 (7.94)	7.69
^3J(HH)	H8C3C4H10	8.65	0.75	2.41	0.18	0.11					0.01	8.51 (8.65)	7.69
^3J(HH)	H6C2C3H9	5.34	−3.44	−0.10	−0.77	0.09		−4.93	0.20	0.23	0.06	5.35 (6.14)	5.61
^3J(HH)	H8C3C4H11	5.44		−0.93		−0.14		6.58		0.77	0.02	5.50 (6.25)	5.61
^4J(HH)	H6C2O1C5H12	−0.20	−0.26	0.33	0.27	−0.05	−0.03				0.00_5	−0.23	0.10
^4J(HH)	H6C2C3C4H10	−0.17	0.21	−0.12	−0.10	−0.01	−0.01	0.13	0.30	0.02	0.00_3	−0.16	0.10
^4J(HH)	H6C2O1C5H13	−0.58		−0.41		0.14		−0.34		0.12	0.01	−0.55	−0.57
^4J(HH)	H6C2C3C4H11	−0.61	−0.11	−0.02	0.01	−0.01	0.01	0.03	0.03	−0.03	0.04	−0.61	−0.57

[a] CP-DFT/B3LYP/[6s,4p,1d/3s,1p] calculations at B3LYP/6-31G(d,p) geometries. The Fourier expansion given in eq 10 for $^nJ(\phi)$ was used. Coefficients A_i and B_j associated with cos($i\phi$) and sin($j\phi$), respectively, are listed. Constant A_0 corresponds to the average parameter $\langle ^nJ\rangle$ in case of free pseudorotation. All values are in Hz. The numbering of atoms corresponds to that shown in Figure 1. [b] Experimental values (in parentheses) are taken from refs 40 and 41.

is determined by the energy of the E forms at 0 and 180°. For all puckered THF forms investigated a puckering amplitude q (B3LYP: 0.371 ± 0.001; MBPT(2), 0.396 ± 0.002 Å; for details see ref 29) is predicted, which is typical of a free or slightly hindered pseudorotor. The calculated energy barrier for pseudorotation is 0.14 kcal/mol, the corresponding enthalpy barrier ΔH is 0.22 (MBPT(2)) and 0.25 kcal/mol (DFT), respectively. The barrier to planarity, ΔE(inv) (ΔH(inv)), is calculated to be 3.36 (2.94) kcal/mol at B3LYP and 4.46 (4.15) kcal/mol at MBPT(2). These values compare well with the available experimental data[30−39] suggesting a stable C_2-symmetrical T form[30,31,34−36] with a q value of 0.38 ± 0.02 Å,[34] a pseudorotational barrier of <0.5 kcal/mol[30] (0.1−0.2 kcal/mol[32,33]), and inversion barriers of 3.49 (microwave spectroscopy[32]) and 3.86 kcal/mol (far-infrared spectroscopy[31]), respectively. Differing results are only obtained from microwave spectroscopic studies,[32,33] which predict a 4-fold pseudorotational potential and stable C_1-symmetrical forms. However, in

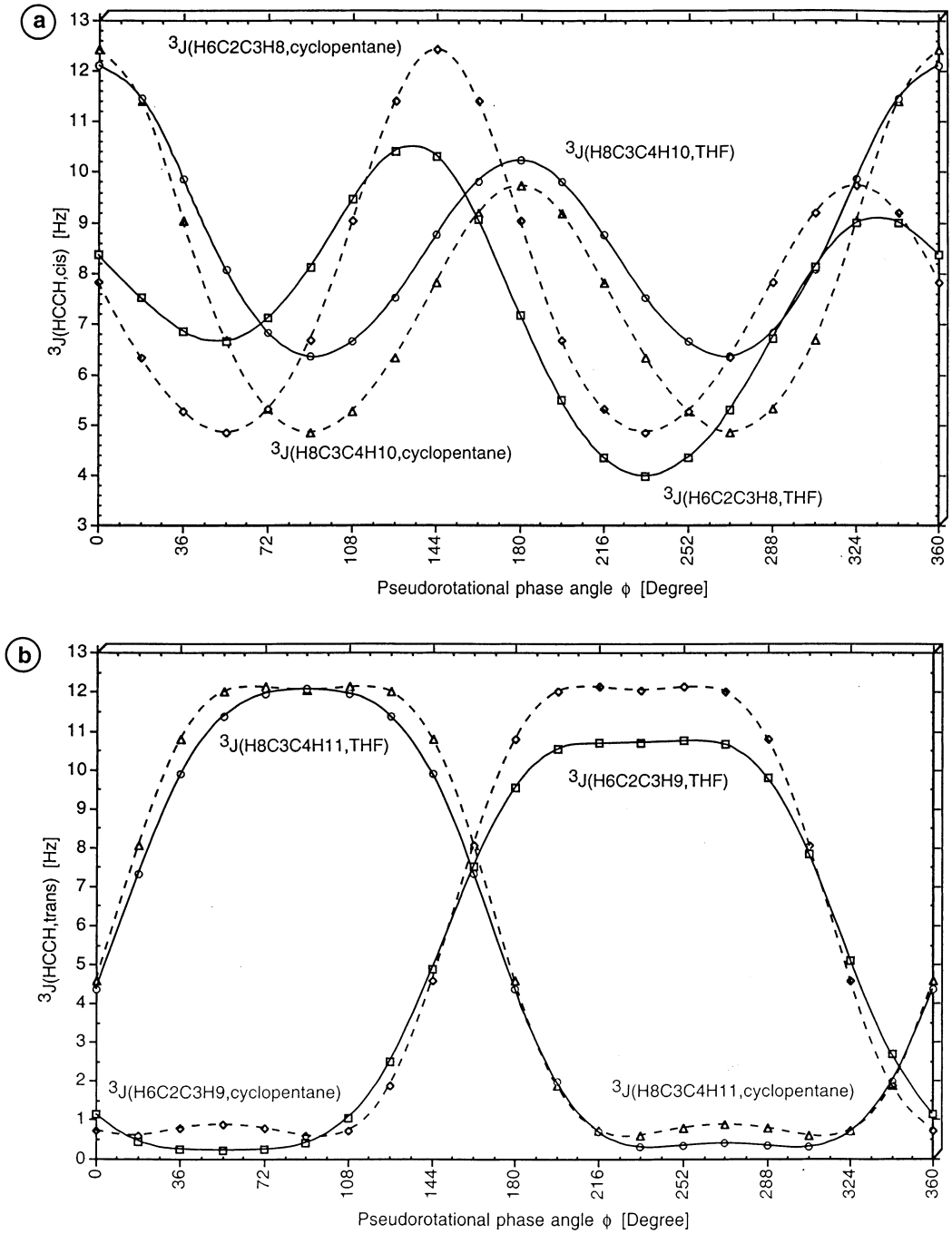

Figure 4. Dependence of the calculated SSCCs ^3J(HCCH) of cyclopentane and THF on the pseudorotational phase angle ϕ (for the definition of J at $\phi = 0°$, see Figure 1). (a) ^3J(HCCH, cis), (b) ^3J(HCCH, trans). CPDFT/[6s,4p,1d/3s,1p] calculations.

these studies, constrained THF models were used, which make results questionable (see below). All previous computational investigations of THF,[37−39] although carried out at lower levels of theory or with smaller basis sets, also predicted a 2-fold pseudorotational potential with C_2-symmetrical T forms at the CES minima.

Details of the calculated equilibrium geometries are discussed elsewhere.[29] Here, we summarize these discussions by stating that both sets of geometries provide a reliable basis for the calculation of the SSCCs. Figure 3 gives the dependence of SSCCs ^3J(HCCH) on the corresponding dihedral angle τ-(HCCH). Clearly, it is not possible to express the dependence of ^3J(HCCH) on the dihedral angle by just one Karplus relationship in a precise way. This however is possible when using the phase angle ϕ in connection with eq 10. In Table 1, the functional dependence of all SSCCs of THF on the pseudorotational phase angle and the calculated average SSCCs of THF are given.

For THF, the vicinal SSCCs ^3J(HCCH) were measured in $CHCl_3$ solution[40] (see Table 1; for a summary of measured SSCCs, see ref 41). The functional dependence of these SSCCs on ϕ is given in Figure 4 and compared with the corresponding SSCC of cyclopentane.

It is obvious from Figure 4 that, despite the different electronic structures of cyclopentane and THF caused by the electronegative O atom and the different steric interactions of eight H atoms in THF compared to ten H atoms in cyclopentane, the Karplus relationships for both molecules are similar. In the case of SSCCs ^3J(HCCH, cis) of cyclopentane, large values are obtained for $\phi = 0$ and 180° (12.4 and 9.7 Hz, Figure 4a)

because for these conformations τ(HCCH) is 0. Smaller values result for $\phi = 90$ or 270° (4.8 Hz) because τ(HCCH) is relatively large in these cases (50°). The ϕ dependence of SSCC ^3J(HCCH, cis) is best represented by a function including four cos $n\phi$ terms (see ref 18). The same functional form is found for the SSCC ^3J(H8C3C4H10, cis) of THF (Figure 4a and Table 1). The Fourier coefficients of the two functions ^3J(HCCH, cis)(ϕ) differ only slightly, and therefore, one could argue that for the structural unit H8C3C4H10 the influence of the O atom is too small to expect large changes in the Karplus relationships of the corresponding ^3J(HCCH, cis) SSCCs.

Similar conclusions can also be drawn for the SSCC ^3J(H6C2C3H8, cis), which becomes more obvious if one shifts the Karplus function for ^3J(H6C2C3H8, cis) by 216° relative to that for ^3J(H8C3C4H10, cis) (see Figure 4a). The functional form possesses now some asymmetry with regard to the center at $\phi = 180°$ but otherwise there is agreement in the way that large values are predicted for the ϕ values 0 and 180° while small values result for 90 and 270°. We conclude that the influence of the O atom does not change the overall form of the Karplus relationship. Accordingly, the calculated $\langle^3J$(HCCH, cis)$\rangle$ values are also similar, namely, 7.69 Hz for cyclopentane and 7.33 and 8.51 Hz for THF (Table 1).

In Figure 4b, the calculated Karplus relationships for the ^3J(HCCH, trans) SSCCs of cyclopentane and THF are shown. Now, the similarity of the three curves is even striking, in particular after shifting the curve for ^3J(H6C2C3H8, trans) by 216°. The influence of the O atom on the trans-SSCCs is much smaller than on the cis-SSCCs, which is due to the fact that the Barfield transmission effect is not operative for the trans coupling pathway.

In Figure 5, perspective drawings of the three-dimensional property surfaces $J(q,\phi)$ (see eq 3; coefficients are given in Table 2) are shown, which were determined by calculating SSCCs of pseudorotating THF for different puckering amplitudes between 0.33 and 0.41 Å and fitting results to eq 3. Functions $J(q,\phi)$ represent the generalization of the Karplus relationship to puckered ring molecules.

The functions $J(\phi)$ shown in Figure 4 correspond to two-dimensional cuts through the surfaces $J(q,\phi)$ for the optimized q value of 0.371 Å. This can be realized by circling on the $J(q,\phi)$ surface of, e.g., ^3J(H6C2C3H9, trans) (compare Figures 4b and 5a). This SSCC possesses a relative small value at $\phi = 0°$, which further decreases for $\phi \rightarrow 90°$. At $\phi = 180°$, ^3J(H6C2C3H9, trans) adopts a relatively large value, which becomes maximal at $\phi = 270°$ and, then, decreases toward a small value at $\phi = 380 = 0°$. The $J(q,\phi)$ surface corresponds to a plane ascending from $\phi = 90°$ toward $\phi = 270°$ (Figure 5a). The plane is distorted slightly into an S-form for large q values (which simply reflects the fact that further increase of puckering leads to little changes in the relevant angles τ(*HCCH*) and the value of ^3J(H6C2C3H9, trans)). The C_s-symmetrical E forms at $\phi = 0$ and 180° possess a similar value of ^3J(H6C2C3H9, trans) as the planar form. The form of the $J(q,\phi)$ surface reveals that ^3J(H8C3C4H9, trans) is not useful to determine the puckering amplitude q of the ring: In the case of free (or nearly free) pseudorotation, the average value of ^3J(H6C2C3H9, trans) is almost independent of q.[18,29]

The $J(q,\phi)$ surface of ^3J(H8C3C4H11, trans) shown in Figure 5b is similar to that of ^3J(H6C2C3H9, trans) where one has to consider that in the latter cases the ϕ-coordinate system is rotated clockwise by 90°. Noteworthy is that all trans SSCCs J(HCCH) of cyclopentane and THF possess a similar $J(q,\phi)$ surface as those shown in parts a and b of Figure 5. The $J(q,\phi)$ surfaces

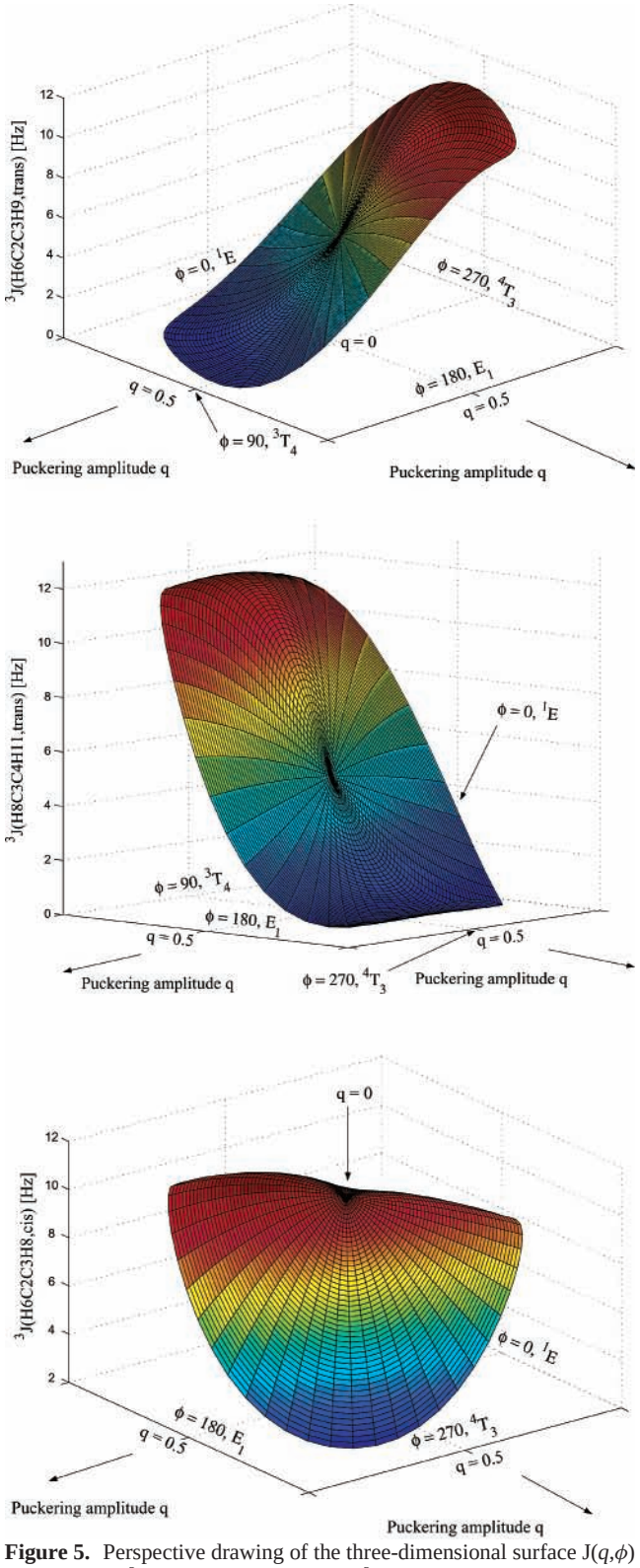

Figure 5. Perspective drawing of the three-dimensional surface $J(q,\phi)$ of SSCCs (a) ^{3}J(H6C2C3H9, trans), (b) ^{3}J(H8C3C4H11,trans), and (c) ^{3}J(H6C2C3H8,cis) of tetrahydrofuran. CPDFT/[6s,4p,1d/3s,1p] calculations. The explicit form of $J(q,\phi)$ is given in Table 2. The direction of radial coordinate q and the angular coordinate ϕ is indicated. Compare with Figure 1. In a, the angle system has been rotated by 90° relative to those in b and c to get a better viewing perspective. In b, $q = 0$ is at the same position as in a, but hidden by the J surface. The same holds for $\phi = 90°$ in c. Colors are given in the order of the rainbow spectrum from large to small J values changing every 2 Hz.

of the SSCCs J(HCCH, cis) are different (see Figure 5c), but they also adopt a similar shape for all SSCCs J(HCCH, cis)

TABLE 2: Generalized Karplus Relationship $^3J(q,\phi)$ for Some Vicinal Proton−Proton Spin−Spin Coupling Constants of THF[a]

		A_0	$A_{1l}\cos(\phi)$	$A_{2l}\cos(2\phi)$	$A_{3l}\cos(3\phi)$	$A_{4l}\cos(4\phi)$	$B_{1l}\sin(\phi)$	$B_{2l}\sin(2\phi)$	$B_{3l}\sin(3\phi)$	STD
^3J(H6C2C3H9, trans)										0.070
		5.312								
A_{k1}/B_{k1}	q	1.481	−17.254	−0.572	0.578	−0.293	−24.078	1.822	−0.080	
A_{k2}/B_{k2}	q^2	−3.790	21.504	0.832	−7.124	1.467	29.090	−3.497	1.873	
^3J(H8C3C4H11, trans)										0.029
		5.020								
A_{k1}/B_{k1}	q	1.906		−3.388		0.466	33.343		−0.818	
A_{k2}/B_{k2}	q^2	−2.070		2.469		−2.264	−42.070		7.783	
^3J(H6C2C3H8, cis)										0.038
		10.253								
A_{k1}/B_{k1}	q	−2.938	1.697	0.593	−0.143	0.294	7.943	−3.549	0.113	
A_{k2}/B_{k2}	q^2	−12.971	−1.492	2.323	1.522	−1.703	−10.499	−5.657	0.888	
^3J(H8C3C4H10, cis)										0.012
		12.48								
A_{k1}/B_{k1}	q	−4.594	4.938	3.716	−0.292	−0.483				
A_{k2}/B_{k2}	q^2	−15.370	−7.815	7.475	2.051	2.120				

[a] CP-DFT/B3LYP/[6s,4p,1d/3s,1p] calculations at B3LYP/6-31G(d,p) geometries. All coefficients are in Hz. The numbering of atoms corresponds to that shown in Figure 1.

investigated for cyclopentane and THF. Similar relationships between the $J(q,\phi)$ surfaces can be found for other SSCCs provided they are of the same type. Different structural environments or the influence of substituents do not change the form of the $J(q,\phi)$ surfaces in a qualitative sense. This finding we have exploited when developing the DORCO method.

In the following, we will use the relationships $J(q,\phi)$ and $J(\phi)$ calculated for cyclopentane and THF to apply the DORCO method described in section 2.

5. Application of the DORCO Method to *cis*- and *trans*-Dimethoxytetrahydrofuran

For the purpose of testing the applicability of the DORCO method, we first use measured vicinal proton,proton SSCCs $\langle^3J(\text{HCCH})\rangle$ of THF (see Table 1) in combination with the calculated functions $^3J(\phi)$ for the same SSCCs to determine the conformation of THF. The activation enthalpy for pseudorotation of THF is calculated to be just 0.2 kcal/mol, and therefore, the probability distribution function should give only a slight preference of the T forms located at the $\phi = 90$ and 270° (see previous section). In view of the C_{2v} symmetry of planar THF, the CES and the probability distribution function must comply with this symmetry; that is, functions $V(q,\phi)$ and $\rho(q,\phi)$ can only contain cos 2ϕ and cos 4ϕ terms. Hence, one needs only to determine coefficients C_2 and C_4 of eq 7.

In Figure 6, probability distribution functions obtained with the procedure described above are shown for three different situations: (a) The measured proton−proton SSCCs $\langle^3J(\text{HCCH})\rangle$ are analyzed using functions $^3J(\phi)$ calculated in this work. A 4-fold pseudorotational potential with stable THF forms at $\phi =$ 46, 134, 226, and 314° is obtained. The analysis shows that the result is dominated by the large error between measured and calculated $\langle^3J(\text{HCCH, trans})\rangle$ values (Table 1) where the latter value is dominated by the constant A_0 (see eq 10). For the purpose of minimizing the difference between the experimental $\langle^3J(\text{HCCH, trans})\rangle$ value and the corresponding A_0 value (for fixed A_2 and A_4 with $|A_2| > |A_4|$), the magnitude of the coefficient C_4 has to become larger than that of C_2. A 4-fold pseudorotational potential results (Figure 6a). (b) If the discrepancy between measured and calculated $\langle^3J(HCCH)\rangle$ values is annihilated by setting

$$A_0(\text{new}) = A_0 + (J_{\text{exp}} - \langle J\rangle) \qquad (12)$$

a 2-fold pseudorotational potential results with maxima of the probability distribution function (minima of the potential) at $\phi = 90$ and 270° (Figure 6b), which is in line with the calculated $V(q,\phi)$ potential. The probability distribution function shows also that the population of the various THF forms differs only slightly because of the small pseudorotational barriers. (c) Test b reveals that the method described will become very sensitive to errors in the calculated $\langle^3J(\text{HCCH})\rangle$ values if the pseudorotational barriers are small. Hence, for sufficiently large pseudorotational barriers, the sensitivity of results to errors in the calculated SSCCs should largely vanish. To prove this point, we repeated the calculation of $\langle^3J(\text{HCCH})\rangle$ values for an assumed pseudorotational barrier of 3 kcal/mol. The probability distribution function shown in Figure 6c correctly predicts the T forms at $\phi = 90$ and 270° to be most populated (most stable) despite the fact that there is still a discrepancy between measured and calculated $\langle^3J(\text{HCCH})\rangle$ values, which leads in test a to the erroneous pseudorotational potential.

It is noteworthy in this connection that microwave studies by Engerholm and co-workers[32] carried out in the late 1960 and repeated and extended by Meyer and co-workers in the 1990[33] suggest a 4-fold pseudorotational potential (V_{4l} coefficients dominate the CES function rather than the V_{2l} coefficients) with equivalent minima at $\phi = 0 \pm 52.5°$ and $180 \pm 52.5°$, which are close to the T forms at $\phi =$ 54, 126, 234, and 306°. The microwave studies use frequency splittings (because of tunneling) and rotational constants and a constrained geometrical model of THF to determine the pseudorotational potential. Because there are more internal coordinates to determine the geometry of THF than measured spectroscopic parameters, several bond lengths and bond angles had to be assumed, for example the CO bond length C2O1 and C5O1 were assumed to be equal and identical to 1.427 Å.[33] If the averaged bond length of C2O1 and C5O1 differs from this fixed value, the minimum is shifted to a THF form of lower symmetry, which automatically leads to a 4-fold rather than 2-fold pseudorotational potential. This is similar as in the case of test a above and casts doubts on the usefulness of the microwave results. It would be better to base the microwave investigation on the quantum chemical model of THF calculated in this work, which would exclude drastic errors because of ill-defined constraints.

The discussion shows that any substituted THF compound can be investigated with the method described provided (a) the pseudorotational barrier is substantially larger than that of THF and (b) a set of SSCCs has been reliably measured. Both criteria

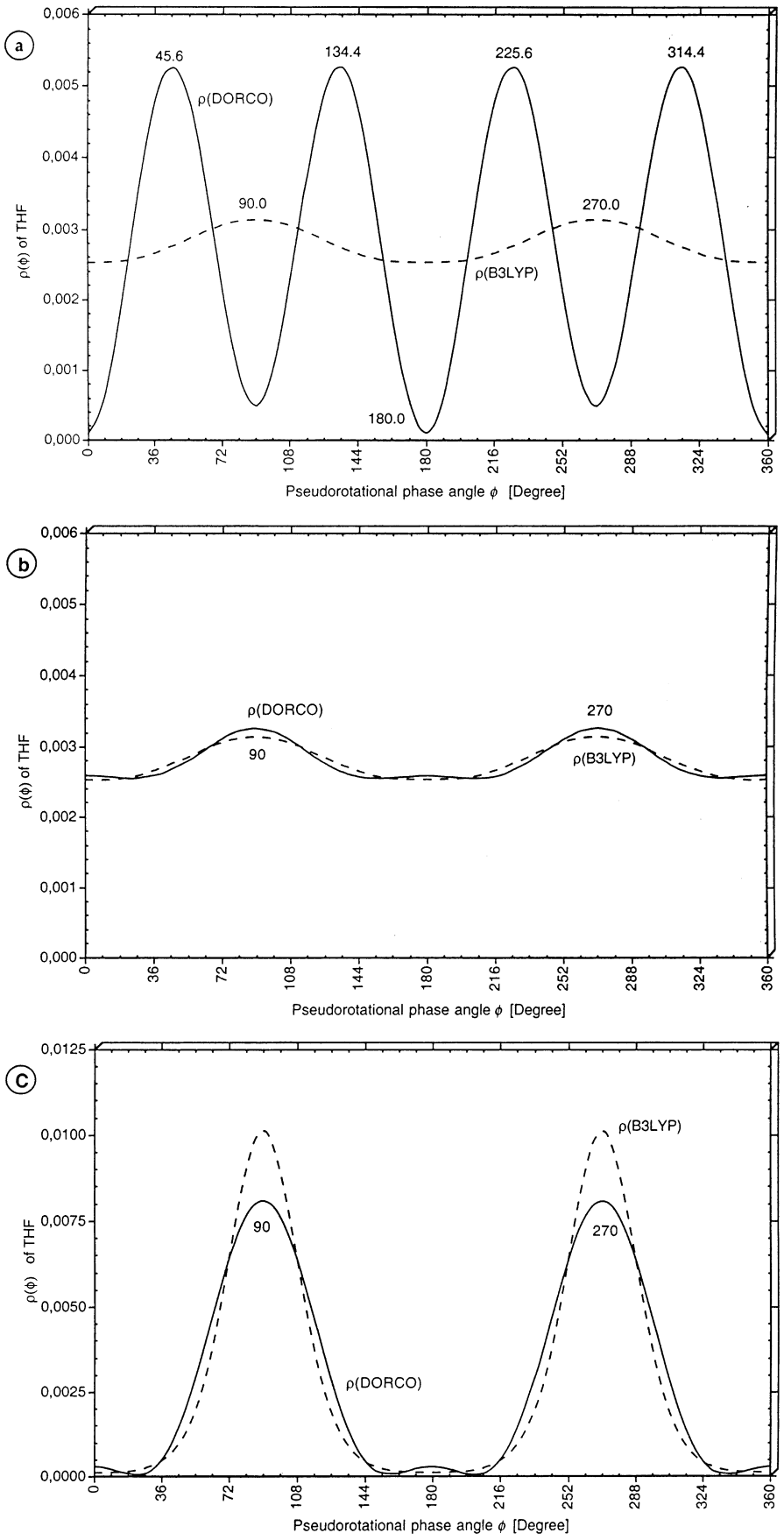

Figure 6. Conformational probability distribution function $\rho(\phi)$ of THF calculated with the DORCO method for three different situations (solid lines): (a) The measured proton−proton SSCCs $\langle^3J(\mathrm{HCCH})\rangle$ of THF are used in connection with the functions $^3J(\phi)$ calculated in this work (see Table 1). (b) Differences between measured and calculated $\langle^3J(\mathrm{HCCH})\rangle$ values are annihilated according to eq 12. (c) The same as a, but the pseudorotational barrier of THF is raised to 3 kcal/mol. In each case, the DORCO probability distribution function is compared with the B3LYP/6-31G(d,p) probability function (dashed lines).

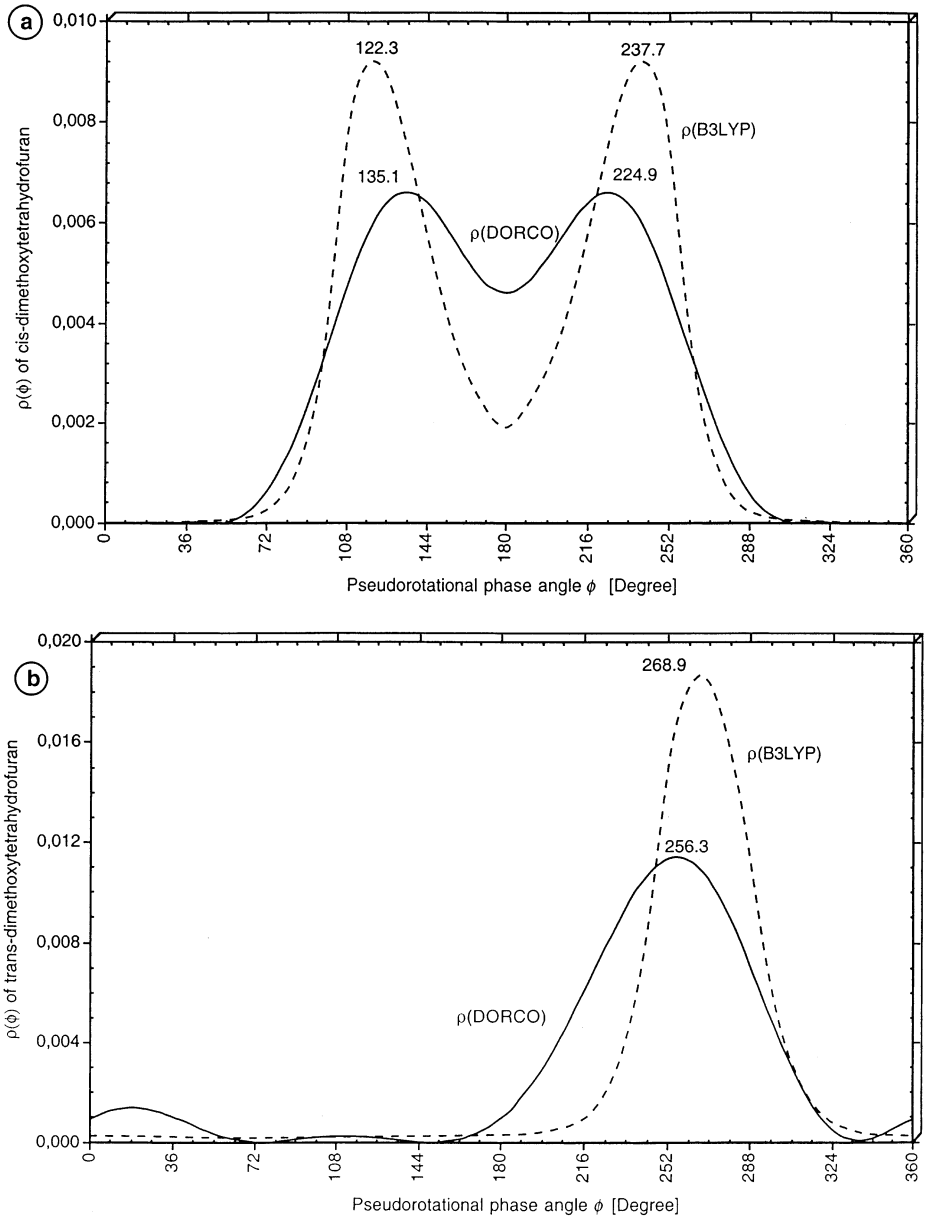

Figure 7. Conformational probability distribution function $\rho(\phi)$ as calculated by the DORCO method (solid line) and by B3LYP/6-31G(d,p) (dashed line). (a) *cis*-2,5-Dimethoxy-tetrahydrofuran and (b) *trans*-2,5-dimethoxy-tetrahydrofuran. The ϕ values of the energy minima (= maxima of $\rho(\phi)$) are given in each case.

TABLE 3: Measured Vicinal Proton−Proton Spin−Spin Coupling Constants ^{3}J(HH) in Hz for *cis*- and *trans*-2,5-Dimethoxytetrahydrofuran[a]

	trans-2,5 dimethoxy-THF	*cis*-2,5 dimethoxy-THF
J(H7C2C3H8,trans)	0.90	2.75
J(H7C2C3H9,cis)	5.10	5.60
J(H8C3C4H10,cis)	8.25	8.40
J(H8C3C4H11,trans)	1.43	6.43
J(H9C3C4H10,trans)	11.98	6.43
J(H9C3C4H11,cis)		9.71

[a] Taken from ref 42.

are fulfilled for *cis*- and *trans*-2,5-dimethoxytetrahydrofuran. In Table 3, the vicinal proton−proton SSCCs $\langle^3J\rangle$ measured for these compounds[42] are listed. They can be used in connection with the corresponding Karplus relationships determined for THF (see Table 1). The planar form of *cis*- and *trans*-2,5-dimethoxytetrahydrofuran would possess C_1 symmetry if the methoxy groups would be differently oriented relative to the ring, e.g., one endo and one exo-oriented. In this way, one of the methoxy groups could interact with the ring O atom, whereas the other has to take an exo-position to avoid steric crowding. A priori these possibilities could not be excluded, and therefore, a total of seven coefficients C_1, C_2, C_3, C_4, D_1, D_2, and D_3 were determined using the following information: six (cis derivative; trans derivative: five) measured $\langle^3J(\mathrm{HCCH})\rangle$ values and three constraints, namely, (a) the condition that $\rho(\phi)$ is always positive, (b) the condition that $\rho(\phi)$ must be normalized to 1, (c1) that for the cis derivative conformations with $\phi = 0 + \Delta$ turn out to be the mirror image of conformations with $\phi = 0 - \Delta$ (see Figure 1; this condition implies C_s symmetry for the planar form and for conformations $^1E(\phi = 0)$ and $E_1(\phi = 180)$, which was confirmed by calculations), and (c2) that for the trans-derivative conformations $^1E(\phi = 0)$ and $E_1(\phi = 180)$ are identical (see Figure 1; this condition does not necessarily imply C_2 symmetry for these forms or the planar form).

In the case of the cis derivative, the sin terms dropped out due to C_s symmetry of the CES, whereas for the trans-derivative,

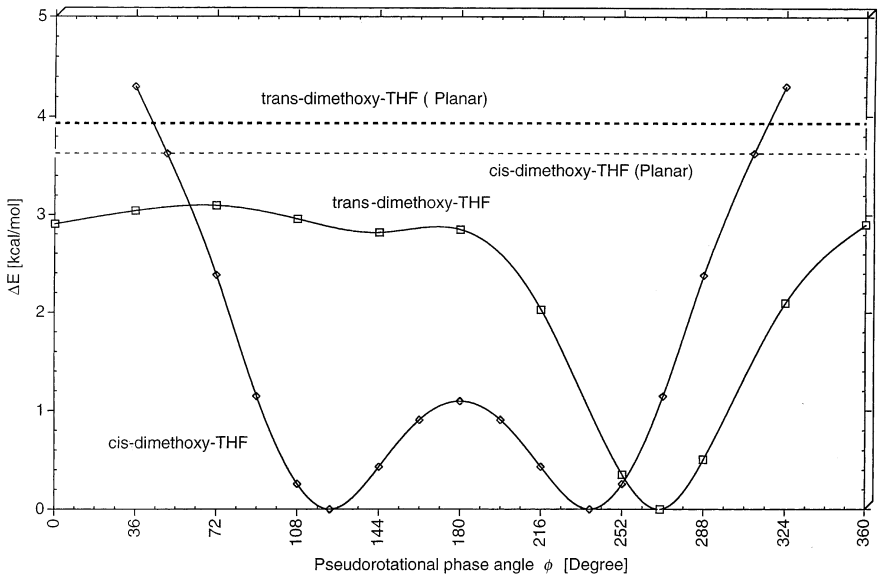

Figure 8. Pseudorotational potential of *cis*- and *trans*-2,5-dimethoxy-tetrahydrofuran. The inversion barriers are indicated by dashed lines (see text). B3LYP/6-31G(d,p) calculations. Note that for the cis derivative puckered forms collapse to the planar form for $\phi = 0 \pm \Delta$ ($\Delta < 36°$). In the case of $\Delta = 36$ or 324°, there is a small energy barrier preventing puckered forms to collapse to the planar form.

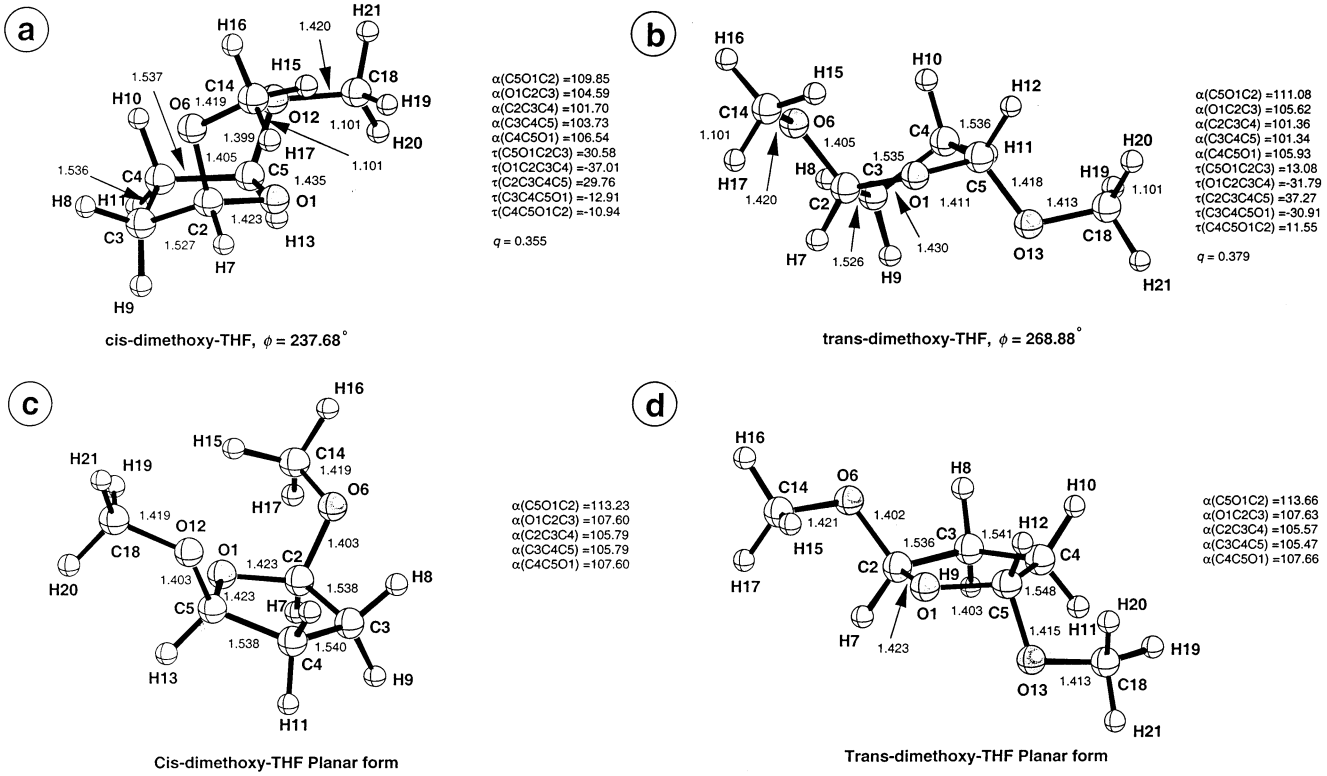

Figure 9. B3LYP/6-31G(d,p) geometries of *cis*- and *trans*-2,5-dimethoxy-tetrahydrofuran. Bond lengths are in Å, and bond angles are in degree. Note that for the cis derivative the second stable conformation at $\phi = 122.3°$ is related to that at $\phi = 237.7°$ by an image-mirror image relationship.

all seven coefficients were included into the function $\rho(\phi)$. The conformational probability distribution functions $\rho(\phi)$ of the two THF derivatives calculated in this way are shown in parts a and b of Figure 7. For the purpose of checking the results of Figure 7, we also calculated the function $V(\phi)$ for *cis*- and *trans*-2,5-dimethoxytetrahydrofuran (Figure 8). From this, we obtained the quantum chemical (directly calculated) conformational probability distributions also shown in parts a and b of Figure 7 (dashed lines).

For the cis derivative, maxima of $\rho(\phi)$ are found at $\phi = 135.1°$ and 224.9°, which agree reasonable with the position of those maxima of the B3LYP/6-31G(d,p) distribution ($\phi = 122.3°$ and 237.7°, Figure 7a). However, the latter maxima are higher possessing a smaller half-width than those obtained with the DORCO method, which simply reflects the somewhat lower accuracy of the DORCO method (deviation of calculated from measured SSCCs). Hence, the cis derivative possesses a 2-fold pseudorotational potential with minima close to forms $^5T_4$ and $^2T_3$, which have the substituents in a more axial position. Optimal bond staggering leads to stabilization of the forms $E_4/^5T_4$, $E_3/^2T_3$, $^3E/^3T_2$, and $^4E/^4T_5$ (see Figure 1). However, conformations $^5T_4$ and $^2T_3$ benefit in addition by a *domino*−*anomeric* effect (for reviews on the anomeric effect, see ref 43) starting at O12 [shortening of C5O12: 1.399 (relative to C2O6);

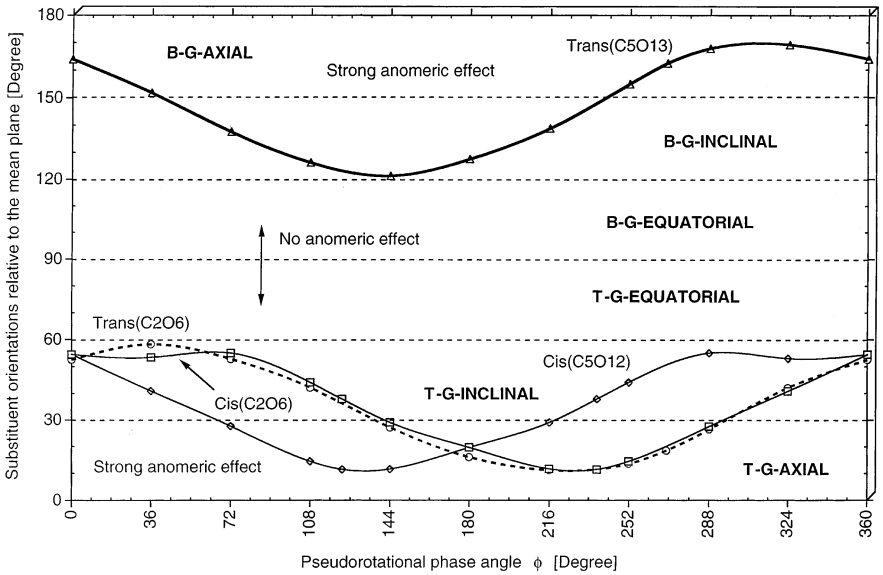

Figure 10. Position of the dimethoxy substituents for *cis*- and *trans*-2,5-dimethoxy-tetrahydrofuran as obtained by B3LYP/6-31G(d,p). For the definition of the substituent positions, see ref 13. The suffixes t and b identify the top and bottom side of the ring (g: geometrical). Note that for the cis derivative puckered forms in the region $\phi = 0 \pm \Delta$ ($\Delta < 36°$ do not exist. In this range, $q = 0.25$ Å was assumed to complete the curves shown.

TABLE 4: Substituent Orientations of *cis*-2,5-Dimethoxytetrahydrofuran and *trans*-2,5-Dimethoxytetrahydrofuran[a]

	cis-2,5-dimethoxy-THF		*trans*-2,5-dimethoxy-THF	
ϕ	C2O6	C5O13	C2O6	C5O12
0	35.3	35.3	52.5	163.9
36	53.4	40.9	58.2	151.7
72	55.0	27.7	52.8	137.5
108	44.1	14.5	42.1	126.1
144	29.1	11.6	27.2	121.2
180	19.7	19.7	16.1	127.4
216	11.7	29.1	11.2	138.7
252	14.5	44.1	13.6	154.9
288	27.6	55.0	26.5	167.8
324	40.8	53.0	42.0	169.2
122.32	11.5	37.9		
237.68	37.9	11.5		
268.88			18.5	162.4

[a] All angle values are in deg. The substituent orientation angle α is given for each bond for a number of selected ϕ values. Values $0° \le \alpha \le 30°$ define axial positions on the topside (t) of the ring (t−g axial), $150° \le \alpha \le 180°$ define bottomside (b) axial positions (b−g axial); $30° < \alpha < 60°$ t−g-inclinal positions, $120° < \alpha < 150°$ b−g-inclinal positions, $60° \le \alpha \le 90°$ t−g-equatorial positions, and $90° < \alpha \le 120°$ b−g-equatorial positions. See ref 13 and compare with Figure 10.

lengthening of C5O1: 1.435 (relative to O1C2)], proceeding to O1 [shortening of O1C2: 1.423 (relative to O1C5); lengthening of C2O6: 1.405 (relative to C5O12)], and ending at O6 [shortening of O6C14: 1.419 (relative to O12C18); lengthening of C14H17: 1.101, see Figure 9a]. The average value of the CO ring bonds (cis: 1.429; trans: 1.421 Å) compares well with the CO bond length of THF (1.428[29]) or that of oxane (1.423 Å[43b]). The domino−anomeric effect is responsible for the position of the two energy minima of the cis form close to 126 and 234°, respectively. A similar domino effect is not possible for the forms close to $\phi = 72°$ and 288°.

Anomeric effects are responsible for a substantial increase of the relative energy of *cis*-2,5-dimethoxytetrahydrofuran for $\phi \rightarrow 0$. The puckering amplitude decreases to zero and at $\phi = 36°$ the relative energy of the planar form is reached. For the region $\phi = 0 \pm 36°$, puckered ring forms of *cis*-2,5-dimethoxy-tetrahydrofuran do not exist; that is, the molecule carries out large amplitude librations relative to the minima at $\phi = 122.3°$ and 237.7°. The energetically most favored process corresponds to a combination of libration and ring inversion; that is, a minimum-energy path for pseudorotation does not exist.

For *trans*-dimethoxytetrahydrofuran, both the DORCO method and B3LYP/6-31G(d,p) calculations predict an asymmetric pseudorotational potential with just one stable conformation (one CES minimum) close to the $^4T_3$ at $\phi = 270°$ (Figure 7b). This overall result is in line with conclusions drawn from a NMR spectroscopic investigation of the trans derivative.[42] Again, the function $\rho(\phi)$ obtained with the DORCO method has a smaller and broader amplitude at the maximum than the directly calculated one (see Figure 7b). As in the case of the cis derivative, this reflects the errors in the calculated SSCCs. The DORCO method predicts the maximum of $\rho(\phi)$ at $\phi = 256.3°$, whereas B3LYP/6-31G(d,p) theory suggests a maximum at $\phi = 268.9°$ (dashed line in Figure 7b).

The conformational minimum for the trans derivative is again influenced by bond staggering of the external ring bonds, which should be better for the T forms at $\phi = 90$ and 270° than for the E forms at $\phi = 0$ and 180°. However, closer inspection reveals that the dominating electronic factor determining the conformational behavior of the trans derivative is again a domino−anomeric effect. The difference of 3 kcal/mol for the T forms at $\phi = 90°$ and 270° results from the different positioning of the methoxy substituents, which can be quantified by calculating the substituent positions according to a procedure described by Cremer.[13] They are listed in Table 4 and show that for $\phi = 270°$ the methoxy substituents are in a more axial and for $\phi = 90°$ in a more equatorial position (Figure 10). Consequently, they are in a better orientation for the former form to support anomeric delocalization and stabilization. This is clearly reflected by the sequence of long and short CO bonds in the unit C−O−C−O−C−O−C (see Figure 9).

6. Conclusions

In this work, we developed the DORCO method to determine the most stable conformations of puckered rings by a comparison of measured and calculated SSCCs. The DORCO method extensively uses the ring puckering coordinates of Cremer and

Pople[11] to express the properties of a pseudorotating puckered ring. In the case of NMR SSCCs, this leads to an extension of the Karplus relationship to puckered rings. In the case of puckered five-membered rings, the general Karplus relationships adopts the form $^nJ(q,\phi)$ or $^nJ(\phi)$. It was shown that in particular the Karplus equations for the vicinal SSCCs ^3J(HCCH)(ϕ) retain their overall form when the ring molecule is substituted. Hence, it is possible to determine $^nJ(\phi)$ for the parent molecule by appropriate quantum chemical calculations and to use this function in connection with measured SSCCs of the substituted ring to determine the conformational probability distribution function of the latter. For this purpose, the conformational probability distribution function of the substituted molecule is expressed, as any other property, as a function of the pseudorotational angle.

The advantages of the DORCO method are the following: (a) Use of the ring puckering coordinates makes it possible to identify a given conformation with the help of NMR measurements in an unique way. (b) Contrary to previous methods, which consider just an equilibrium between two (a few) conformational minima, DORCO determines the conformational probability distribution function ρ for a larger region in the conformational space. (c) DORCO includes the condition $\rho \geq 0$ right from the beginning and in this way avoids unphysical results (e.g., $\rho(\phi) < 0$ and oscillations in $\rho(\phi)$) typical of other procedures. (d) The method can be applied to any puckered *N*-membered ring. (e) The mathematical procedure of DORCO guarantees the best possible fit of the true conformational probability distribution function. (f) All SSCCs or other properties of a ring molecule (NMR chemical shifts, rotational constants, vibrational frequencies, etc.) sensitive to conformational changes can be used in connection with DORCO.

The DORCO method was applied to THF and two of its derivatives. Geometries of puckered THF forms and the pseudorotational CES of THF were accurately described at both the DFT/B3LYP/6-31G(d,p) and MBPT(2)/levels of theory. Using calculated THF geometries, CP-DFT/B3LYP calculations with the [6s,4p,1d/3s,1p] basis set provided SSCCs in reasonable agreement with the available experimental values. The complete set of the 26 SSCCs of pseudorotating THF was determined and expressed as functions of the two ring puckering coordinates q and ϕ. For the first time, Karplus relationships $^nJ(\phi)$ and $^nJ(q,\phi)$ were systematically derived for THF. Averaging of J over the pseudorotational motion led to values $\langle ^nJ\rangle$ directly comparable with measured values.

In the case of THF, the DORCO method will lead to reasonable results if deviations of calculated from measured $\langle ^nJ\rangle$ values are empirically corrected. This is necessary because of the very small pseudorotational barrier (0.14 kcal/mol) of THF that implies a very flat conformational probability distribution function. However, as soon as the pseudorotational barrier adopts values of 1 kcal/mol and more these corrections are no longer needed. For *cis*- and *trans*-2,5-dimethoxytetrahydrofuran, the pseudorotational minima were determined with the help of DORCO. It was shown that the phase angle ϕ and by this the type of ring pucker can be determined with an accuracy of 4% or better ($\Delta\phi = 13°$).

The importance of a domino−anomeric effect for the stability of 2,5-dimethoxytetrahydrofuran was demonstrated. This leads to pseudorotational barriers of 3 (trans derivative) and 3.6 kcal/mol (cis derivative). However, in the case of *cis*-2,5-dimethoxytetrahydrofuran, the energetically most favored process corresponds to a combination of libration and ring inversion rather than pure pseudorotation as in the case of the trans derivative.

The procedure developed in this work provides a basis to investigate the conformational behavior of puckered ring molecules with the help of NMR measurements and quantum chemical calculations. Work is in progress to apply the DORCO method using NMR chemical shifts.

Acknowledgment. This work was supported at Göteborg by the Swedish Natural Science Research Council (NFR). Calculations were done on the supercomputers of the Nationellt Superdatorcentrum (NSC), Linköping, Sweden. D.C. thanks the NSC for a generous allotment of computer time.

Supporting Information Available: Geometries and calculated energies for THF forms along the pseudorotational path. This material is available free of charge via the Internet at http://pubs.acs.org.

References and Notes

(1) See, for example: *Encyclopedia of Nuclear Magnetic Resonance*; Grant, D. M., Harris, R. K., Eds.; Wiley: Chichester, U.K., 1996; Vol 1−8.
(2) (a) Kowalewski, J. *Prog. NMR Spectrosc.* **1977**, *11*, 1. (b) Kowalewski, J. *Ann. Rep. NMR Spectrosc.* **1982**, *12*, 81.
(3) Contreras, R. H.; Facelli, J. C. *Ann. Rep. NMR Spectrosc.* **1993**, *27*, 255.
(4) Contreras, R. H.; Peralta, J. E. *Prog. NMR Spectrosc.* **2000**, *37*, 321.
(5) (a) Karplus, M.; Anderson, D. H. *J. Chem. Phys.* **1959**, *30*, 6. (b) Karplus, M. *J. Chem. Phys.* **1959**, *30*, 11.
(6) Karplus, M. *J. Am. Chem. Soc.* **1963**, *85*, 2870.
(7) (a) Altona, C. In *Encyclopedia of Nuclear Magnetic Resonance*; Grant, D. M., Harris, R. K., Eds.; Wiley: Chichester, U.K., 1996; p 4909. (b) Altona, C.; Sundaralingam, M. *J. Am. Chem. Soc.* **1973**, *95*, 2333. (c) Haasnoot, C. A. G. *J. Am. Chem. Soc.* **1993**, *115*, 1460.
(8) Sychrovsky, V.; Gräfenstein, J.; Cremer, D. *J. Chem. Phys.* **2000**, *113*, 3530.
(9) (a) Becke, A. D. *J. Chem. Phys.* **1993**, *98* 5648. (b) Becke, A. D. *Phys. Rev. A* **1988**, *38*, 3098. (c) Lee, C.; Yang, W.; Parr, R. P. *Phys. Rev. B* **1988**, *37*, 785.
(10) Helgaker, T.; Watson, M.; Handy, N. C. *J. Chem. Phys.* **2000**, *113*, 9402.
(11) Cremer, D.; Pople, J. A. *J. Am. Chem. Soc.* **1975**, *97*, 1354.
(12) Cremer, D.; Szabo, K. J. In *Methods in Stereochemical Analysis, Conformational Behavior of Six-Membered Rings, Analysis, Dynamics, and Stereoelectronic Effects*; Juaristi, E., Ed.; VCH Publishers: New York, 1995; p 59.
(13) Cremer, D. *Isr. J. Chem.* **1980** *20*, 12.
(14) Cremer, D. *J. Phys. Chem.* **1990**, *94*, 5502.
(15) (a) Cremer, D. *Acta Crystallogr. B* **1984**, *40*, 498. (b) Essen, H.; Cremer, D. *Acta Crystallogr. B* **1984**, *40*, 418.
(16) Cremer, D. *Isr. J. Chem.* **1983**, *23*, 72.
(17) Cremer, D. *J. Chem. Phys.* **1979**, *70*, 1898; 1911; 1928.
(18) Wu, A.; Cremer, D.; Auer, A.; Gauss, J. *J. Phys. Chem. A* **2002**, *106*, 657.
(19) (a) de Leeuw, F. A. A. M.; Altona, C.; Kessler, H.; Bermel, W.; Friedrich, A.; Krack, G.; Hull, G. *J. Am. Chem. Soc.* **1983**, *105*, 2237. (b) Haasnoot, C. A. G.; de Leeuw, F. A. A. M.; de Leeuw, H. P. M.; Altona, C. *Biopolymers* **1981**, *20*, 1211.
(20) Džakula, Ž.; Derider, M.; Markley, J. L. *J. Am. Chem. Soc.* **1996**, *118*, 12796.
(21) (a) Džakula, Ž.; Westler, W. M.; Edison, A. S.; Markley, J. L. *J. Am. Chem. Soc.* **1992**, *114*, 6195. (b) Džakula, Ž.; Edison, A. S.; Westler, W. M.; Markley, J. L. *J. Am. Chem. Soc.* **1992**, *114*, 6200.
(22) Hariharan, P. C.; Pople, J. A. *Theor. Chim. Acta* **1973**, *28*, 213.
(23) For a recent review, see: Cremer, D. In *Encyclopedia of Computational Chemistry*; Schleyer, P. v R., Allinger, N. L., Clark, T., Gasteiger, J., Kollman, P. A., Schaefer, H. F., Schreiner, P. R., Eds.; Wiley: Chichester U.K.; Vol 3, 1998; p 1706.
(24) Dunning, T. H., Jr. *J. Chem. Phys.* **1989**, *99*, 1007.
(25) McQuarrie, D. A. *Statistical Thermodynamics*; Harper and Row Publishers: New York, 1973.
(26) Kutzelnigg, W.; Fleischer, U.; Schindler, M. In *NMR−Basic Principles and Progress*; Springer, Heidelberg, 1990; Vol. 23, p 165.
(27) Kraka, E.; Gräfenstein, J.; Gauss, J.; He, Y.; Reichel, F.; Olsson, L.; Konkoli, Z.; He, Z.; Cremer, D. *COLOGNE2000*; Göteborg University: Göteborg, Sweden, 2000.
(28) Frisch, M. J.; Trucks, G. W.; Schlegel, H. B.; Scuseria, G. E.; Robb, M. A.; Cheeseman, J. R.; Zakrzewski, V. G.; Montgomery, J. A., Jr.; Stratmann, R. E.; Burant, J. C.; Dapprich, S.; Millam, J. M.; Daniels, A. D.; Kudin, K. N.; Strain, M. C.; Farkas, O.; Tomasi, J.; Barone, V.; Cossi,

M.; Cammi, R.; Mennucci, B.; Pomelli, C.; Adamo, C.; Clifford, S.; Ochterski, J.; Petersson, G. A.; Ayala, P. Y.; Cui, Q.; Morokuma, K.; Malick, D. K.; Rabuck, A. D.; Raghavachari, K.; Foresman, J. B.; Cioslowski, J.; Ortiz, J. V.; Stefanov, B. B.; Liu, G.; Liashenko, A.; Piskorz, P.; Komaromi, I.; Gomperts, R.; Martin, R. L.; Fox, D. J.; Keith, T.; Al-Laham, M. A.; Peng, C. Y.; Nanayakkara, A.; Gonzalez, C.; Challacombe, M.; Gill, P. M. W.; Johnson, B. G.; Chen, W.; Wong, M. W.; Andres, J. L.; Head-Gordon, M.; Replogle, E. S.; Pople, J. A. *Gaussian 98*, revision A.5; Gaussian, Inc.: Pittsburgh, PA, 1998.

(29) Wu, A.; Cremer, D. *Int. J. Mol. Sci.* In press.

(30) Lafferty, W. J.; Robinson, D. W.; Louis, R. V., St.; Russell, J. W.; Strauss, H. L. *J. Chem. Phys.* **1965**, *42*, 2915.

(31) Davidson, R.; Warsop, P. A. *J. Chem. Soc., Faraday Trans. 2* **1972**, *68*, 1875.

(32) Engerholm, G. G.; Luntz, A. C.; Gwinn, W. D.; Harris, D. O. *J. Chem. Phys.* **1969**, *50*, 2446.

(33) Meyer, R.; Lopez, J. C.; Alonso, J. L.; Melandri, S.; Favero, P. G.; Caminati, W. *J. Chem. Phys.* **1999**, *111*, 7871.

(34) Geise, H. J.; Adams, W. J.; Bartell, L. S. *Tetrahedron* **1969**, *25*, 3045.

(35) Lugar, P.; Buschmann, J. *Angew. Chem., Int. Ed. Engl.* **1983**, *22*, 410.

(36) David, W. I. F.; Ibberson, R. M. *Acta Crystallogr., Sect. C* **1992**, *48*, 301.

(37) Cremer, D.; Pople, J. A. *J. Am. Chem. Soc.* **1975**, *97*, 1358.

(38) Han, S. J.; Kang, Y. K. *J. Mol. Struct. (THEOCHEM)* **1996**, *369*, 157.

(39) (a) Diez, E.; Palma, J.; San-Fabián, J.; Guilleme, J. *J. Comput. Chem.* **1988**, *9*, 189. (b) Siri, D.; Gaudel, A.; Tordo, P. *THEOCHEM* **2002**, *582*, 171.

(40) Lambert, J. B.; Papay, J. J.; Khan, S. A.; Kappauf, K. A.; Magyar, E. S. *J. Am. Chem. Soc.* **1974**, *96*, 6112.

(41) Kalinowski, H. O.; Berger, S.; Braun, S. *^{13}C NMR-Spektroskopie*; Thieme: Stuttgart, Germany, 1984.

(42) Gagnaire, D.; Vottero, P. *Bull. Soc. Chim.* **1972**, 873.

(43) (a) Kirby, A. J. *The Anomeric Effect and Related Stereoelectronic Effects at Oxygen*; Springer, New York, 1983. (b) For a recent update on the literature concerning the anomeric effect, see: Cuevas, G.; Juaristi, E. *J. Am. Chem. Soc.* **2002**, 13088.